Virology 489 (2016) 128–140

Contents lists available at ScienceDirect

Virology

journal homepage: www.elsevier.com/locate/yviro

Development of a sheep challenge model for Rift Valley fever

Bonto Faburay [a], Natasha N. Gaudreault [a], Qinfang Liu [a], A. Sally Davis [a], Vinay Shivanna [a], Sun Young Sunwoo [a], Yuekun Lang [a], Igor Morozov [a], Mark Ruder [b], Barbara Drolet [b], D. Scott McVey [b], Wenjun Ma [a], William Wilson [b], Juergen A. Richt [a,*]

[a] Department of Diagnostic Medicine/Pathobiology, College of Veterinary Medicine, Kansas State University, Manhattan, Kansas, Unites States
[b] United States Department of Agriculture, Agricultural Research Service, Arthropod Borne Animal Disease Research Unit, Manhattan, Kansas, United States

ARTICLE INFO

Article history:
Received 28 September 2015
Returned to author for revisions
3 December 2015
Accepted 8 December 2015
Available online 31 December 2015

Keywords:
Rift Valley fever
Sheep
Challenge model
Rift Valley fever virus
Strains
Viremia

ABSTRACT

Rift Valley fever (RVF) is a zoonotic disease that causes severe epizootics in ruminants, characterized by mass abortion and high mortality rates in younger animals. The development of a reliable challenge model is an important prerequisite for evaluation of existing and novel vaccines. A study aimed at comparing the pathogenesis of RVF virus infection in US sheep using two genetically different wild type strains of the virus (SA01-1322 and Kenya-128B-15) was performed. A group of sheep was inoculated with both strains and all infected sheep manifested early-onset viremia accompanied by a transient increase in temperatures. The Kenya-128B-15 strain manifested higher virulence compared to SA01-1322 by inducing more severe liver damage, and longer and higher viremia. Genome sequence analysis revealed sequence variations between the two isolates, which potentially could account for the observed phenotypic differences. We conclude that Kenya-128B-15 sheep infection represents a good and virulent challenge model for RVF.

Introduction

Rift Valley fever virus (RVFV) is a mosquito-borne zoonotic pathogen within the genus *Phlebovirus*, family *Bunyaviridae*. Although large outbreaks have predominantly occurred in sub-Saharan Africa, recent outbreaks outside of the African continent, in the Arabian Peninsula, have raised concerns about the potential spread of the virus to Europe, Asia and the Americas (Balkhy and Memish, 2003; Bird et al., 2009; Chevalier et al., 2010; Pepin and Tordo, 2010). Human infections with RVFV are associated with acute febrile illness that in some cases can progress to more severe disease, including retinal vasculitis resulting in blindness, encephalitis and hepatitis resulting in fatal hemorrhagic fever (Bird et al., 2009). Case fatality rates as high as 20–50% have been reported (Heald, 2012; Nguku et al., 2010). In sheep, goats and cattle, the disease is characterized by abortion storms and high rates of mortality in young animals (Coetzer, 1977, 1982; Pepin and Tordo, 2010). Due to concerns about its potential use as a biological weapon, RVFV is categorized as a high priority agent by the National Institute for Allergy and Infectious Diseases (NIAID), Centers for Disease Control and Prevention (CDC) and the U.S. Department of Agriculture (USDA).

Because of the presence of experimentally proven competent vectors, there is a high risk for introduction and establishment of RVFV in the US (Iranpour et al., 2011; Turell et al., 2008, 2010). Currently, there are no fully licensed RVFV vaccines in the US for either livestock or human use. Therefore, development of an effective vaccine represents an important area of research and availability of a challenge model is an important prerequisite for the development, evaluation, and licensing of future vaccines. To date, several RVFV animal infection models have been described in non-human primates (Miller et al., 2002; Smith et al., 2012), mice (Busquets et al., 2014; Flick and Bouloy, 2005; Ikegami and Makino, 2011; Linden et al., 2015; Smith et al., 2010; Tomori and Kasali, 1979), hamsters and rats (Easterday, 1965; Findlay, 1932; Flick and Bouloy, 2005; Linden et al., 2015; Miller et al., 2002), and more recently in sheep and goats (Busquets et al., 2010; Weingartl et al., 2014). Also, two types of challenge models have been employed for vaccine efficacy studies: the pregnancy model, which requires effective synchronization of pregnancy in host species (Bird et al., 2011), and the viremia model, which is affected by lack of consistency due to variation in individual host animal responses (Drolet et al., 2012; Fagbami et al., 1975; Kortekaas et al., 2012). Ideally, the development of an RVF vaccine designed for use in livestock should be tested in its natural host species, i.e. in ruminant livestock. Although sheep are the livestock most susceptible to RVFV infection, there is lack of detailed information about the impact of various sheep breed differences on clinical responses to experimental RVFV infection, data which are

* Corresponding author.
E-mail address: jricht@vet.k-state.edu (J.A. Richt).

http://dx.doi.org/10.1016/j.virol.2015.12.003
0042-6822/

vital for vaccine efficacy study design. A challenge model for both sheep and goats was recently described (Weingartl et al., 2014). In these studies, different breeds of sheep (Suffolk cross, Rideau Arcott cross, Ile-de-France cross with Rideau Arcott) were inoculated with a RVFV strain (ZH501) isolated in 1977 in Egypt. These and other authors found that the clinical and pathological outcome of experimental RVFV infections in ruminants is very much dependent on the strain of RVFV used for inoculation, the species, breed and age of the host animals.

Different strains of RVFV have been responsible for numerous disease outbreaks in Africa and in the Arabian Peninsula. The Kenya-128B-15 (Ken06) strain was isolated from a mosquito during the Kenya 2006/2007 outbreak, which resulted in significant human and livestock mortalities (Sang et al., 2010). The SA01-1322 (SA01) strain was isolated from a mosquito during the Saudi Arabia 2000/2001 outbreak (Miller et al., 2002), which resulted in more than 200 human deaths and significant loss of livestock (Al-Hazmi et al., 2003; Arishi et al., 2000; Madani et al., 2003). These strains represent distinct genetic isolates and we hypothesized that they would have phenotypic differences with different clinical and pathological outcomes in infected susceptible livestock.

The aim of this study was to compare sheep infection with two strains of RVFV, Ken06 and SA01, in order to obtain relevant clinical and pathological data for subsequent evaluation of experimental vaccines. Here we describe the establishment of a small ruminant challenge model for RVF using sheep and two genetically distinct RVFV strains.

Results

Rectal temperatures

In the first study in Dorper x Katahdin sheep inoculated with 1×10^6 PFU of SA01 or Ken06 rectal temperatures were measured taken daily on 0–10, 14 and 21 days post infection (dpi). Rectal temperatures showed transient increases from baseline with the highest increase for both experimental groups (Ken06 and SA01) occurring at 2 dpi (Fig. 1A). There were significant differences in mean rectal temperatures between baseline, 0 dpi (SA01 = 39.8 °C, Ken06 = 39.7 °C, $n=6$) and 2 dpi (SA01 = 40.8 °C, Ken06 = 41.1 °C, $n=6$) for animals inoculated with either RVFV strains ($P<0.05$). No significant change from baseline occurred in the mock-inoculated control group ($n=2$) during the length of the study. Also the observed mean temperature differences between the virus inoculated and mock- inoculated groups on 2 dpi were statistically significant ($P<0.01$). There was no significant difference in mean rectal temperatures between SA01 and Ken06 inoculated groups at 2 dpi ($P>0.05$).

Polypay sheep ($n=5$) inoculated with 2×10^6 PFU of Ken06 in the second study showed variable temperature responses (Fig. 1B). Peak temperatures were observed on 1 or 2 dpi (range = 40.1–41.9 °C), with an increase in all sheep ($n=4$), except for sheep #45, which showed an unusual decline in temperature from 1 to 3 dpi then increase at 4 dpi. Three sheep, #41, #43 and #44, maintained high temperatures (41.2 °C, 41.9 °C, 41.4 °C, respectively) at 2 dpi, whereas sheep #42 had a lower temperature at 2 dpi. Thereafter, animals showed transient increase and decrease in temperature until 10 dpi, the study endpoint (Fig. 1B).

Mortality

There was no mortality in the first study in the Dorper x Katahdin sheep. However, of the 5 Polypay sheep inoculated with the higher dose of Ken06 virus, 3 animals (#41, #45, #44) died at 3, 4 and 5 dpi of acute RVFV infection.

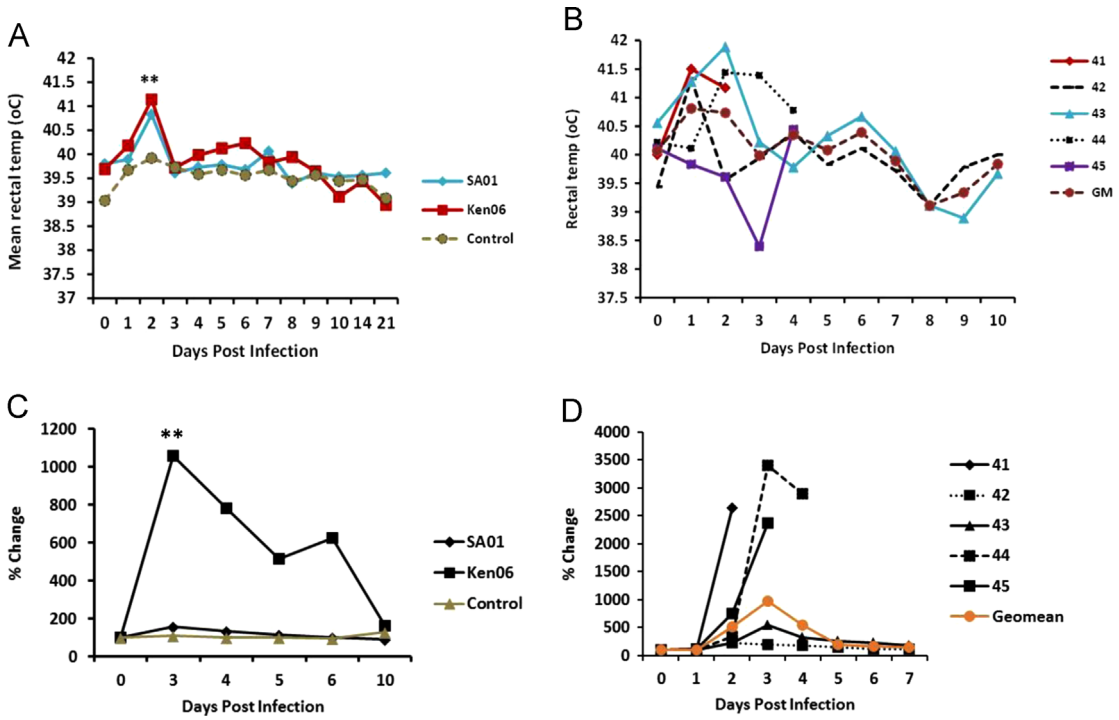

Fig. 1. Kinetics of rectal temperatures of sheep inoculated with RVFV SA01 and Ken06 (A) and sheep inoculated with a higher dose of Ken06; ** denotes mean rectal temperatures of SA01 and Ken06 inoculated sheep are significantly higher than mock inoculated sheep ($P<0.01$), (B) GM = group mean, (C) shows percentage change of the geometric mean AST values for the different groups of sheep inoculated with the two different wild type strains of RVFV; **denote AST values of Ken06 inoculated sheep are significantly different from SA01 or mock-inoculated sheep ($P<0.001$), (D) shows percentage change in individual AST and geometric mean (Geomean) AST values for sheep ($n=5$) inoculated with 2×10^6 pfu of Ken06;

Blood chemistry and hematology

Analyses of blood chemistry values were performed for levels of albumin, ALP, GGT, AST and BUN. No significant changes in the levels of albumin, ALP and GGT following viral inoculation were found and consequently description of the analyses focused on the levels of AST and BUN, as they appeared to be the most affected by RVFV infection. Increased AST levels are indicative of hepatocellular damage while BUN increases are associated with renal damage. The AST levels were measured on day 0 through day 10 pi. In the first study, a dramatic increase in mean percentage change of enzyme level was observed for the Ken06 inoculated group at 3 dpi followed by a steady decrease beginning at day 4 dpi to normal or near normal baseline levels by 10 dpi (Fig. 1C). The SA01 inoculated group showed a slight but non-significant increase at 3 dpi compared to the mock inoculated control group ($P > 0.05$). The mean percent changes in the AST levels were significantly higher in animals inoculated with Ken06 compared to those inoculated with SA01 or the control group ($P < 0.001$). The Ken06 strain induced a peak mean increase at 3 dpi of 1059% in the inoculated animals, whereas SA01 only induced a peak mean increase of 160%; the control animals remained statistically unchanged (Fig. 1C). Of the 5 sheep inoculated with the higher dose of Ken06, 3 sheep (#41, #44, #45) responded with a more dramatic elevation of AST levels (Fig. 1D). Interestingly, all of these sheep with a dramatic AST increase were found dead within 1–2 days after its observation. The BUN concentrations were tested on 0, 3, 4, 5, 6 and 10 dpi and showed a peak level for both viruses at 3 dpi. The mean concentrations at 3 dpi, 5 dpi, 6 dpi and 10 dpi were significantly higher than values at 0 dpi (baseline values, $P < 0.05$) for sheep inoculated with either strain of the virus. BUN values of non-infected control animals did not change significantly ($P = 0.451$). The BUN concentrations returned to near baseline levels by 10 dpi, the sampling endpoint. Similar kinetics for BUN values were observed in sheep inoculated with the higher dose of Ken06 strain (data not shown). The mean WBC levels varied when compared with baseline but no significant trends increases or decreases in virus inoculated animals were found (data not shown).

Viremia

Virus was detectable in the serum starting at 1 dpi by both real-time RT-PCR (Fig. 2A) and virus plaque assay (Fig. 2B). By 2 dpi, all virus-inoculated sheep were viremic (Fig. 2A and B). Peak viremia determined by virus titration occurred in sheep infected with Ken06 at 2 and 3 dpi (Fig. 2B). Peak viremia for SA01 sheep occurred at 2 dpi (Fig. 2B). Sheep infected with the SA01 strain were all negative by both real-time RT-PCR (Fig. 2A) and plaque assay by 5 dpi (Fig. 2B). Sheep inoculated with the Ken06 strain were negative by real-time RT-PCR (Fig. 2A) at 7 dpi and by plaque assay (Fig. 2B) at 6 dpi. Control sheep sera remained negative for virus-specific markers throughout the study. In the follow up study with 5 Polypay sheep inoculated with a higher dose of the Ken06 strain, similar viral kinetics were observed with peak viremia of sheep at 2 dpi (Fig. 2C and D). These results were consistent with the first study except Ct values at 3 dpi were slightly lower (Fig. 2C–D).

Viral load or titers in tissues

In the virus comparison study, brain, liver, spleen and bile samples collected at necropsy were tested for virus presence by virus isolation. Ken06 was isolated from the liver at 3 and 4 dpi (Fig. 3B), and from the spleen from 3 out to 21 dpi (Fig. 3D). SA01 was isolated from the liver at 3 dpi (Fig. 3B), and from the spleen at 3, 5 and 6 dpi (Fig. 3D). Virus isolation at 3 and 4 dpi in liver and spleen correlated with the low *Ct* values detected in the liver and spleen tissues of Ken06 infected sheep on the same days by RT-PCR (Fig. 3A and C). No virus was isolated from the brain or bile

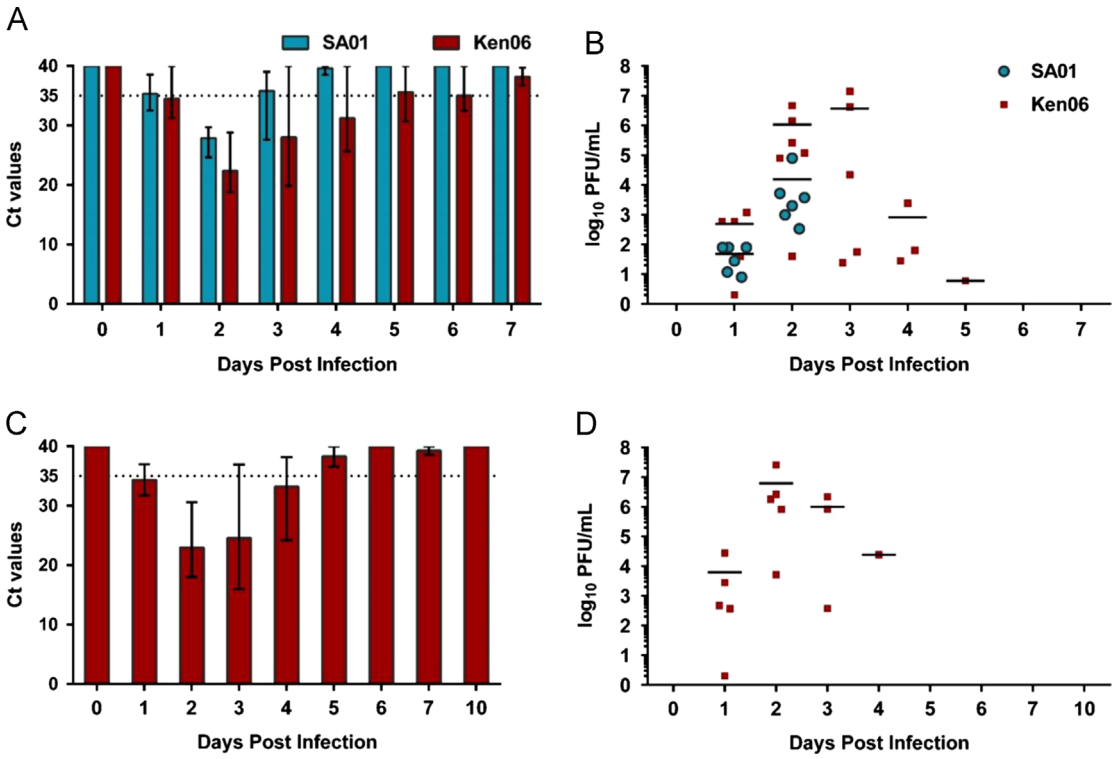

Fig. 2. Virus titration and RNA levels in sheep sera. The mean with the range of *Ct* values (A) or viral titers (B) for virus positive sheep serum are shown. Panel (C) and (D) represent mean *Ct* values and viral titers, respectively, obtained from serum of sheep inoculated with the higher dose of Ken06. To be considered positive by real-time RT-PCR, the *Ct* value for at least 2 of the 3 RVF genome segments must be less than or equal to 35 (represented by a dashed line).

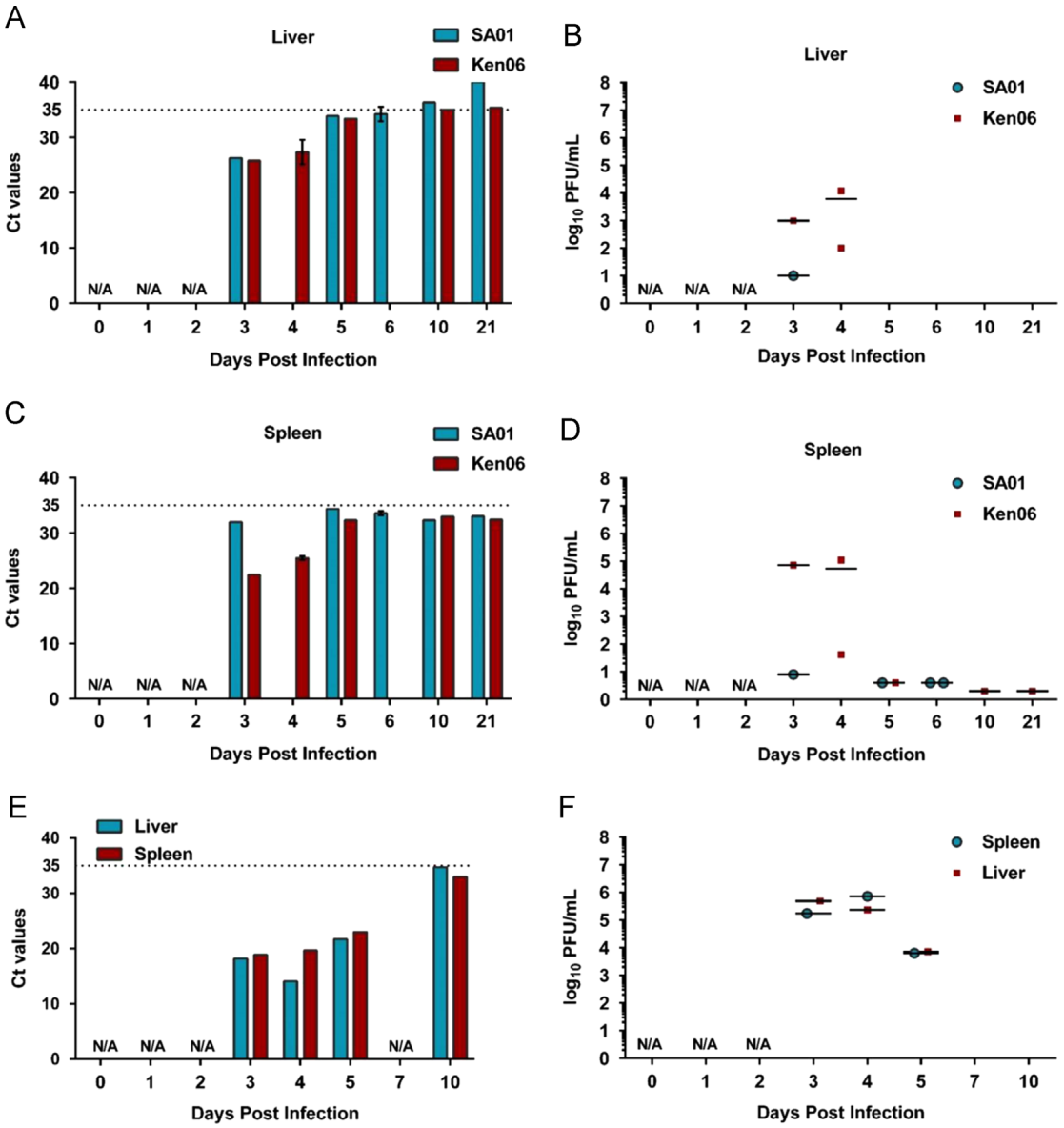

Fig. 3. Virus titrations and RNA levels of various tissues after RVFV infection. Mean *Ct* values obtained from liver tissue samples (A) and virus titers obtained from the liver (B) of sheep inoculated with SA01 and Ken06; mean *Ct* values for spleen tissue samples (C) and virus titers obtained from the spleen (D). Bottom panels show mean Ct values for liver and spleen tissue samples (E) and virus titers of isolates from the liver and spleen (F) of sheep inoculated with the higher dose of Ken06 strain. Necropsies were not performed on days 0, 1, 2 or 7 post inoculation (N/A).

samples collected from the infected sheep, or in any tissues sampled from the control sheep. All nasal swabs collected from sheep inoculated with the SA01 strain were negative by RT-PCR. At 4 dpi low levels (<2 $\log_{10}$ pfu/ml) of virus were isolated from the nasal swabs of 3 out of the 6 sheep infected with the Ken06 strain. In the later study with the higher dose of Ken06 strain, virus was isolated from the liver and spleen (Fig. 3F) of inoculated sheep at 3, 4 and 5 dpi. Higher viral titers in both tissues were observed. No nasal swabs were collected during the second, Ken06 only, study.

Serological responses

ELISA serologic responses are presented in Fig. 4. In the first study, sera obtained from animals in both experimental groups, SA01 and Ken06, had increased antibody activity against the RVFV N and Gn proteins as indicated by ELISA from 5 to 21 dpi (Fig. 4A and B). The overall trend showed a time-dependent increase in the level of total IgG response with peak responses occurring at 21 dpi (Fig. 4A and B). N-specific antibody responses had higher *OD* values compared to the Gn-specific responses (Fig. 4A and B). In the Ken06 only study, onset of seroconversion as measured by IgG response in the N-specific ELISA was at 5 dpi, with a time-dependent increasing antibody response until study endpoint at 10 dpi. Seroconversion in the Gn-specific ELISA was detected at 10 dpi. The non-vaccinated sheep did not seroconvert (Fig. 4C).

Results of the plaque reduction neutralization assay for the first study are shown in Table 1. Three (3) out of 6 animals in the SA01-infected group and 4 out of 6 in the Ken06-infected group had detectable neutralizing antibody titers (titer=10) at 3 dpi; one animal inoculated with Ken06 developed a detectable neutralizing titer at 2 dpi. At 4 dpi, 4 out of 5 animals inoculated with SA01 and Ken06 developed mean neutralizing antibody titers of 15 and 20, respectively (Table 1). All virus inoculated sheep developed neutralizing antibody titers by 5 dpi. The neutralizing antibody titers increased steadily through 21 dpi for all animals reaching titration end point levels (titer=1280) at 9 dpi for the Ken06-infected

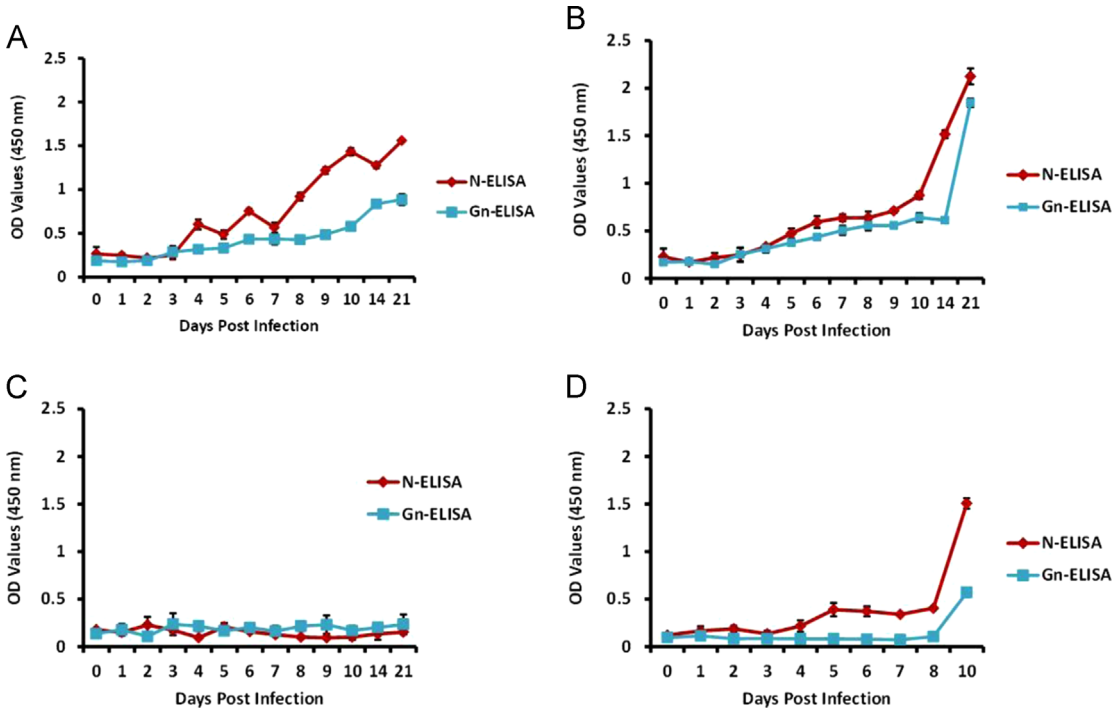

Fig. 4. Specific indirect ELISA shows kinetics of total IgG antibody responses in sheep inoculated with wild type RVFV strains, SA01 (A) (cut-off for Gn-ELISA=0.308, N-ELISA=0.321) and Ken06 (B) (cut-off for Gn-ELISA=0.239; N-ELISA=0.483), C shows responses in non-infected control sheep, D shows IgG responses in sheep inoculated with increased dose (2×10^6) of Ken06 strain (cut-off for Gn-ELISA=0.14, N-ELISA 0.192).

Table 1
Reciprocal $PRNT_{80}$ titers in sheep infected with RVFV strains, SA01 and Ken06.

Sheep no.		*Reciprocal $PRNT_{80}$ titers*												
	Virus strain	*Days: 0 preinf*	*1 pi*	*2 pi*	*3 pi*	*4 pi*	*5 pi*	*6 pi*	*7 pi*	*8 pi*	*9 pi*	*10 pi*	*14 pi*	*21 pi*
54	SA01	–	–	–	10									
65	SA01	–	–	–	–	10	20	80						
58	SA01	–	–	–	–	–	40							
59	SA01	–	–	–	–	10	40	80						
60	SA01	–	–	–	10	20	80	160	640	640	320	1280		
61	SA01	–	–	–	10	20	80	80	160	320	1280	> 1280	> 1280	> 1280
Mean					10[a]	15[b]	52	100	400	480	800	1280	1280	1280
63	Ken06	–	–	–	–									
62	Ken06	–	–	–	10	10								
64	Ken06	–	–	–	10	20	40							
55	Ken06	–	–	–	10	10								
68	Ken06	–	–	–	–	–	40	80	80	640	1280	> 1280		
69	Ken06	–	–	10	10	40	80	320	1280	> 1280	> 1280	> 1280	> 1280	1280
Mean					10[b]	20[b]	53	200	680	960	1280	1280	1280	1280

Key:
preinf=pre-infection; pi=post infection; the blanks for individual animals at the various days pi signify the animals were euthanized before this time point; (–) indicates no neutralizing antibody titers were detected.

[a] $n=3$
[b] $n=4$

group and 10 dpi for the SA01 group. These high antibody titers were maintained in both groups until 21 dpi, the study endpoint (Table 1). Overall, the two different strains elicited similar kinetics of neutralizing antibody response showing no statistically significant differences in the mean neutralizing antibody titers between the two experimental groups ($P > 0.05$). The mock-inoculated control sheep did not develop neutralizing antibody titers. Two of the Polypay sheep inoculated with a higher dose of Ken06 were tested for neutralizing antibody titers on 0, 5, 6, 7, 8 and 10 dpi. Overall, the neutralizing antibody response in the sheep showed similar time-dependent increases in titers, with peak titers detected at 10 dpi, the study endpoint (Table 2).

Genome analysis

Genome sequence analysis of SA01 and Ken06 revealed nucleotide and amino acid variations in the L, M and S segments. The L, M and S segments of Ken06 showed 1.19% (76 mutations), 1.49% (58 mutations) and 1.54% (26 mutations) nucleotide variation, respectively, relative to SA01. At the amino level, in

comparison to SA01, Ken06 strain manifested 11 aa substitutions (0.53% variation) in the L protein, 2 substitutions (1.31% variation) in NSm, 8 substitutions (1.5% variation) in Gn, 2 (0.39% variation) in Gc, and 5 (1.88% variation) in NSs proteins. The N protein was highly conserved between the two strains manifesting no amino acid differences. The two strains clustered in different genetic clades in the phylogenetic tree (Fig. 5).

Pathology

In the first study, comparing SA01 and Ken06, gross pathology observations revealed no consistent pattern of differences between the two virus strains. Necropsies at 3-4 dpi, had the most prominent gross lesions. Livers were diffusely pale with pinpoint tan foci consistent with necrosis disseminated throughout the hepatic parenchyma (Fig. 6A). Animals necropsied on day 5 and 6 were similar to the earlier dpi time-points, although there were decreased numbers of necrotic foci apparent throughout their livers. Petechiae and ecchymoses were present in the hepatic parenchyma some of the early time-point animals, but this was not tied to a single strain or time-point. While gross lesions were absent in livers at later post-infection time-points, livers remained pale throughout the study. Mild splenomegaly was the only other gross lesion attributable to RVFV.

Similar and frequently more severe gross lesions in the liver were appreciated during the second Ken06 only study. The three animals that died acutely had larger necrotic foci as well as multifocal hemorrhage (Fig. 6B). Again, spleen changes, splenomegaly and additionally occasional subcapsular hemorrhages, were seen. Lungs were heavy, wet and multifocally or nearly diffusely dark pink, interpreted as pulmonary edema and congestion. No gross lesions were appreciated at the 10 dpi necropsies in the second study.

Hepatic histopathology scores and immunohistochemistry (IHC) findings are summarized in Table 4 for the virus comparison study and Table 5 for the second study. Hepatic histopathologic changes were present on a background of mild peri-portal lymphoplasmacytic inflammation present in all study animals including uninoculated controls (Fig. 7A and B). RVFV antigen IHC was convincingly negative on uninoculated control liver and the detection system exhibited minimal background (Fig. 7C and D)

Table 2
Reciprocal $PRNT_{80}$ titers in sheep inoculated with 2×10^6 pfu of RVFV Ken06 strain.

Sheep no.	*Reciprocal $PRNT_{80}$ titers*					
	Days: 0 preinf.	*5 pi*	*6 pi*	*7 pi*	*8 pi*	*10 pi*
42	0	80	80	320	640	1280
43	0	80	80	160	320	> 1280
Mean		80	80	240	480	1280

Key: preinf=pre-infection; pi=post infection.

In the virus comparison study, regardless of virus strain and dose, early time-point post-infection sheep livers had similar hepatic histopathology. However, matched time-point Ken06 livers consistently labeled more strongly for RVFV antigen by IHC than SA01 livers (Fig. 7E–L). Hepatic lesions were multifocal yet spared the portal tracts and ranged from foci of predominantly histiocytic inflammation to similar inflammation surrounding necrotic foci filled with cellular debris as well as degenerate and viable neutrophils. The most severe lesions were accompanied by marked amounts of hemorrhage and fibrin thrombi in central veins immediately adjacent to foci of necrosis (Fig. 7 M and N). Hepatic lesions in all acute time-point animals (3–5 dpi) contained hepatocytes and macrophages whose cytoplasm was positive for viral antigen (Fig. 7G,H, K,L and O,P). (Fig. 7M–P). In the virus strain comparison study, there were no hepatic lesions attributable to either virus strain by day 10 with the exception of SA01 animal #61, which had scattered single hepatocyte necrosis accompanied by low numbers of macrophages, all negative for RVFV by IHC. Likewise hepatic lesions were mild in the two animals in the second study that survived until study end point, 10 dpi.

Splenic changes in early time-point post-infection Ken06 animals in the virus comparison study differed from those in the SA01 animals. While lymphoid follicular hyperplasia as well as mild scattered lymphoid follicle depletion was found in all early time-point spleens compared to control animal tissues; the changes in Ken06 animal spleens were more prominent. Additionally, 3 and 4 dpi Ken06 spleens had scattered perifollicular necrosis involving the red pulp which was IHC positive for RVFV antigen. Both SA01 and Ken06 acute time-point animals had lymph node histiocytosis. These lymphoid tissue changes were present and more severe in the three acute time-point second study animals in which we observed multifocal to diffuse lymphoid follicle depletion, red pulp necrosis and fibrin deposition in spleens as well as moderate to marked lymphoid follicle depletion in mesenteric lymph nodes. Multifocally, histiocytes in the sinusoids of these lymph nodes were positive for viral antigen. In the second Ken06 only study, kidney glomeruli often appeared hypercellular and were positive for viral antigen. Similar glomerular changes were observed multifocally in a 4 dpi Ken06 animal in the virus comparison study. Additionally, animal #43 in the second study, euthanized at 10 dpi had multifocal renal tubular necrosis with adjacent lymphoplasmacytic interstitial nephritis. Affected tubular epithelial cells and luminal debris were positive for viral antigen.

Additional lesions were appreciated in other organs. A Ken06 4 dpi animal in the virus comparison study had mild multifocal adrenocortical necrosis in the zona fasciculata that was positive for RVFV antigen. A 10 dpi SA01 and a 21 dpi Ken06 sheep in this study also had occasional glial nodules in cerebral brain parenchyma. Additionally, one Ken06 10 dpi animal had multifocal perivascular lymphohistiocytic inflammation in its brain stem. None of these brain lesions were positive by IHC. Also in multiple early time-point animals for both viral strains we observed small cardiac lesions, i.e. foci of histiocytic and lymphoplasmacytic

Table 3
Liver histopathology score descriptions.

Histopathology Score	*Description*
0	No lesions attributable to Rift Valley Fever virus
1	Multifocal, mid-zonal to central foci of lymphohistiocytic (lymphocytes and macrophages) inflammation with lesser numbers of plasma cells and occasional single hepatocyte necrosis
2	Multifocal, 1–2 mm areas of mid-zonal to central lymphohistiocytic inflammation frequently with central necrosis shifting inflammation to predominantly neutrophils. Less than 5% of examined parenchyma involved
3	As prior but more severe necrotic lesions involving up to 15% of hepatic tissue reviewed. Additionally present is scattered hepatocyte apoptosis.
3+	Greater than 15% of the parenchyma is necrotic and severe multifocal hemorrhage is also present

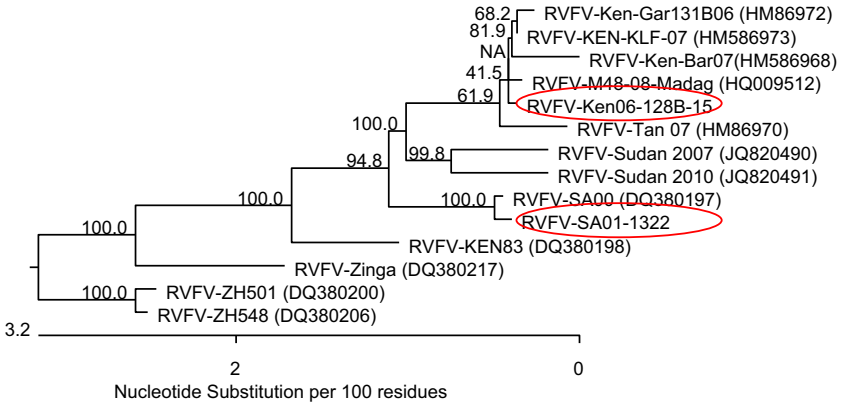

Fig. 5. Phylogenetic analysis of nucleotide sequences of the M segments of various RVFV strains. The phylogenetic tree shows separation of Ken06 and SA01 (circled) into separate clades indicating that the two strains are genetically distinct. NA=not applicable.

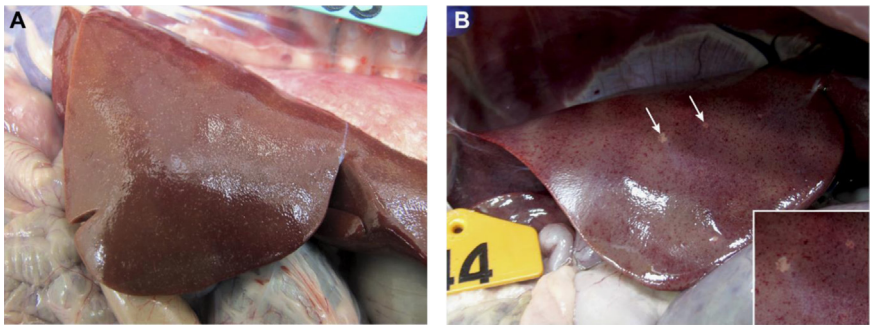

Fig. 6. Gross liver pathology photos of acute post-infection time-point livers *in situ* from virus inoculated cattle were diffusely pale. (A) A virus comparison study animal inoculated with Ken06 and euthanized at 3 dpi, additionally had multifocal 1 mm tan foci (necrosis) disseminated throughout the tissue, (B) the higher dose Ken06 study animal #44 that died 5 days post-inoculation additionally had larger foci of necrosis white "←" and diffuse petechiation.

Table 4
Histopathology and immunohistochemistry for the SA01 and Ken06 comparison study.

Sheep no.	*Virus strain*	*Days PI*	*Avg H Score*	*IHC*	*H Other Organs*	*IHC +*
54	SA01	3	3	+	s	–
58	SA01	5	2	+	h	–
59	SA01	6	2	–	h	–
65	SA01	6	1	–	h,	–
60	SA01	10	0	–	i, b	–
61	SA01	21	1.5	–	h	–
63	Ken06	3	3	+	s	s
62	Ken06	4	3	+	s, h	s
55	Ken06	4	3	+	a	s, a, k
64	Ken06	5	1	+	h	–
68	Ken06	10	0	–	b, e	–
69	Ken06	21	0	–	b	–
70	Mock	21	0	–	–	–
71	Mock	21	0	–	–	–

Avg H Score is average hepatic histopathology score as per Table 3. IHC denotes "+" or "–" liver IHC result. H Other Organs is histopathology in organs other than the liver. IHC + denotes which additional tissues were positive for RVFV antigen. Key: s=spleen, h=heart, i=intestine, b=brain, a=adrenal, e=eye and k=kidney.

inflammation, that were negative for virus antigen by IHC and not virus strain specific. One Ken06 10 dpi animal had aggregates of macrophages and neutrophils in the iridocorneal angle of one eye that were negative for viral antigen. However, we observed no eye lesions in any other sheep including the second study animals. All acute time-point 3-5 dpi second study sheep had multifocal pulmonary edema as evidenced by increased numbers of intra-alveolar macrophages. Finally, the 10 dpi SA01 sheep on the virus comparison study had a prominent intestinal coccidiosis, potentially enhanced by the stress of high containment housing.

Discussion

Understanding the pathogenesis of RVFV infection in susceptible hosts is a prerequisite for developing a reliable challenge model for testing and evaluation of RVF vaccines. Previous studies have focused on strain ZH501, isolated in 1977 in Egypt (Weingartl et al., 2014). In this study, we examined the clinical and pathological outcome of experimental infection with two more recently isolated genetically distinct strains of RVFV, SA01-1322 and Kenya 06-128B-15 (Miller et al., 2002; Sang et al., 2010) in the most susceptible livestock species, the sheep. The results of this study showed that Dorper x Katahdin cross and Polypay breeds of sheep are susceptible to RVFV infection showing viremia upon infection with either strain of the virus (Fig. 2B and D). The viremia induced by both strains in sheep was transient, lasting on average 3 days, with peak levels occurring at 2 and 3 dpi; this was consistent with the gross and microscopic lesions and viral antigen presence in organs.

The detection of viremia coincided with the appearance of fever, at 2 and 3 dpi. Furthermore, virus was isolated from liver and spleen of sheep infected with both strains at multiple time points, from 1–5 dpi. Our overall findings demonstrate that both viral strains induced RVFV clinical signs in both sheep breeds. Viremia is a key metric for vaccine efficacy and for determining host susceptibility to RVFV infection (Bird et al., 2008, 2011; Weingartl et al., 2014; Wilson et al., 2014). The findings in this study suggest susceptibility of both breeds of sheep, Polypay and

the Dorper x Katahdin cross, to RVFV infection and their suitability as an experimental animal for vaccine studies.

Regardless of virus strain and dose, early time-points post-infection multifocal necrosis often accompanied by hemorrhage (Fig. 6A and B) was found in the liver, consistent with gross hepatic lesions reported prior from natural RVF cases in sheep (Daubney and Garnham, 1931; Swanepoel and Coetzer, 1994). In both experimental studies reported here, the hepatic histopathology findings correlated well with the gross findings. The low numbers of peri-portal lymphocytes and plasma cells additionally seen in all livers including those of the uninoculated control animals were negative for viral antigen by IHC and considered to be within normal limits for incidental peri-portal inflammation seen in normal sheep (Fig. 7A–D). RVFV attributable lesions were multifocal yet typically spared the portal tracts and ranged from foci of lympho-histiocytic inflammation to similar inflammation surrounding necrotic foci filled with cellular debris and degenerate and viable neutrophils. The most severe lesions were accompanied by hemorrhage (Fig. 7E–F, I–J and M–N). These lesions frequently contained hepatocytes and macrophages whose cytoplasm was positive for viral antigen (Fig. 7G–H, K–L, and O–P). On average, dpi matched study animals had similar hepatic histopathology. However, the RVFV antigen IHC signal from the Ken06 samples was consistently stronger in these time-point matched samples. Additionally, only Ken06 animals had RVFV IHC positive splenic lesions at 3 and 4 dpi. Acute time-point higher dose Ken06 study animals exhibited a marked increase in their degree of hepatic and splenic

Table 5
Histopathology and immunohistochemistry for the Ken06 only study.

Sheep no.	*Virus strain*	*Days PI*	*H Score*	*IHC*	*H Other Organs*	*IHC +*
41	Ken06	3 died	3+	+	l, s, ln	s, ln
45	Ken06	4 died	3+	+	l, s, ln	s, ln, k
44	Ken06	5 died	3+	+	l, s, ln	s, ln, k
42	Ken06	10	1	–	l, k	–
43	Ken06	10	1	–	k	k

Columns as described for Table 4. Key: +=positive for viral antigen by IHC, –=negative for viral antigen on IHC, l=lung, s=spleen, k=kidney and ln=mesenteric lymph node. * Kidney was not available for animal #41. The liver histopathology score for three of these animals was appreciably higher than a score of 3 in Table 3.

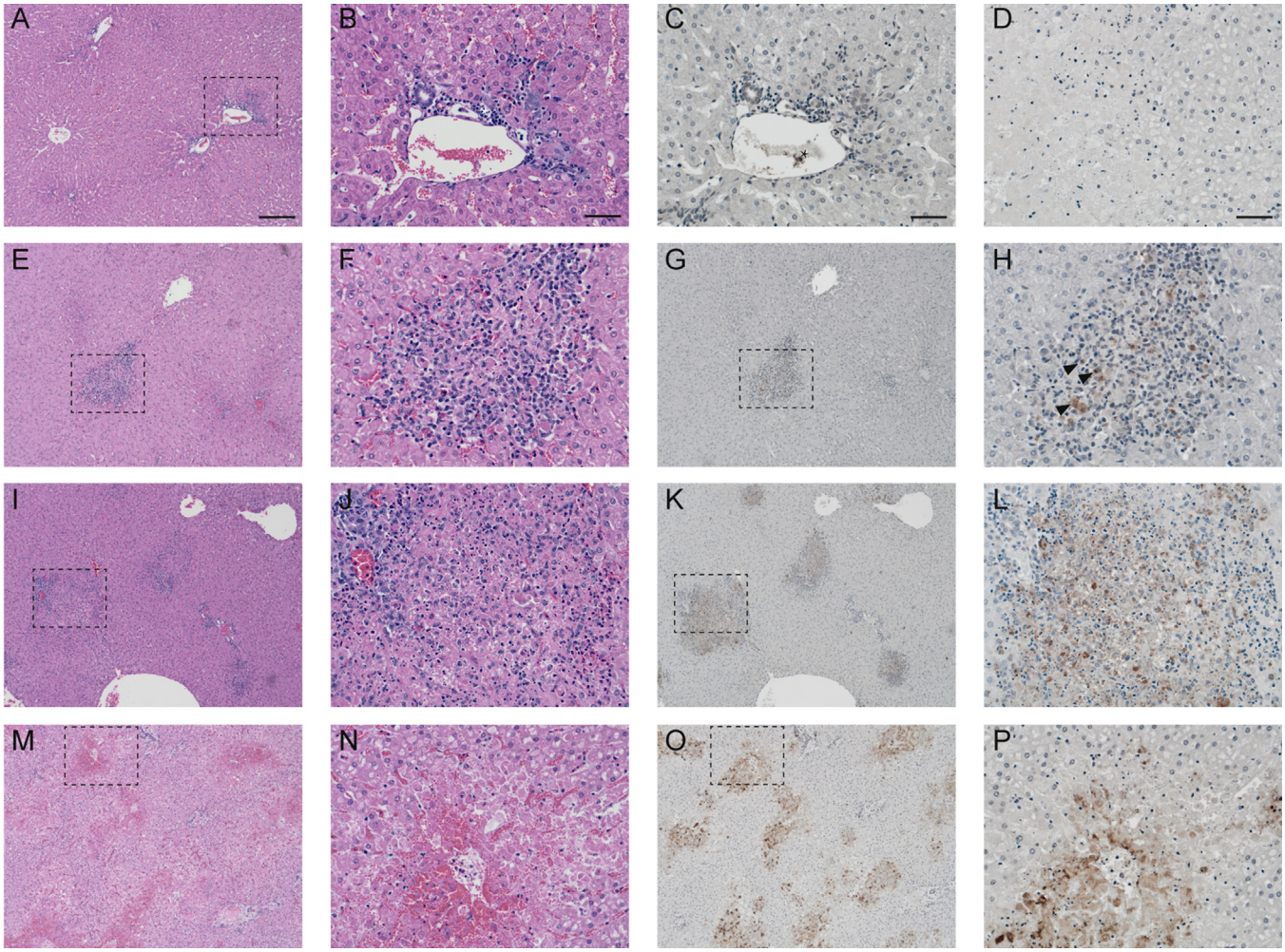

Fig. 7. Acute time-point liver histopathology and immunohistochemistry. (A) and (B) 100x hematoxylin and eosin (H&E) stains of liver parenchyma from a mock inoculated animal. Each broken line box outlines the region shown at 400x magnification in the next image In, (B) white "*" denotes lymphoplasmacytic background inflammation commonly seen in all animal's hepatic portal tracts, (C) Rift Valley fever virus antigen IHC on mock inoculated animal control tissue was negative and (D) background was minimal on the no primary antibody reagent control slide for viral antigen immunohistochemistry (IHC), both 400x. The black star "*" in (C) denotes acid hematin (artifact) seen in some central vein lumens. Row's 2–4 in order left to right: 100x H&E, 400x H&E, IHC for viral antigen at 100x and 400x. Row 2 is from a 3 dpi SA01 inoculated sheep, Row 3 is from a 3 dpi Ken06 inoculated sheep and Row 4 is a second study Ken06 inoculated animal that died 4 dpi. Rift Valley fever virus caused acute mid-zonal to central hepatic necrosis with predominantly neutrophilic and histiocytic inflammation (E–F, I–J and M–N). Additionally, hemorrhage was common within the larger necrosis lesions (M–N). Positive IHC signal in these lesions is the dark brown–red chromogen precipitate in the cytoplasm of hepatocytes, neutrophils and macrophages as well as cellular debris (G–H, K–L, Q–P). The black arrows on (H) denote examples of IHC positive cells. Bars in columns 1 and 3 are 20 μm and bars in columns 2 and 4 are 50 μm.

tissue destruction and positive labeling for RVFV antigen by IHC in comparison to Ken06 animals in the first study, attributable to either the higher viral inoculum dose or change in sheep breed. The second study animals also regularly had kidney changes, commonly glomerular filtration of RVFV antigen and less commonly scattered tubular degeneration and necrosis. Greater understanding of these kidney changes might be gained through additional special stains and use of electron microscopy. The gross and histopathology lesions that we found in both studies including changes in the lymph nodes, adrenal gland, brain, heart and eye were consistent with RVFV lesions reported prior for both natural disease cases in sheep and experimental sheep RVFV inoculations (Daubney and Garnham, 1931; Easterday, 1965; Ikegami and Makino, 2011; Swanepoel and Coetzer, 1994; Rippy et al., 1992). Overall, the lesions were more severe in time-point matched Ken06 animals and these changes were heightened in the second study.

Similar temperature responses were observed in SA01 and Ken06 inoculated sheep in the virus comparison study (Fig. 1A). However, virus was isolated from nasal discharges of sheep infected with Ken06 but not with SA01. Shedding of infectious RVFV in nasal discharges of infected sheep has not been widely documented in the scientific literature (Busquets et al., 2014; Nicholas et al., 2014), and detection of the virus in the nasal discharges of sheep inoculated with Ken06 could be an indication of high virulence and upper respiratory tropism of this virus. Mock inoculated control sheep housed alongside the challenged animals remained negative throughout the study, suggesting the virus was not shed at adequate levels for transmission to occur among the sheep. Although RVFV is most often transmitted through infected mosquito bites, the potential for transmission through nasal discharge should not be entirely ruled out. However, in all of our RVFV infection trials so far, we have not observed non-infected control animals housed together with experimentally infected animals becoming infected or seroconverting. Additional evidence for higher virulence for Ken06 when compared to SA01 is the detection of consistently higher percentage increases in AST levels in animals inoculated with this strain (Fig. 1C and D). The increase levels of this liver enzyme in the serum signifies hepatocellular damage in the affected animals (Smith et al., 2012), and the level of increase may be indicative of the severity of the damage. Additionally, 3 of the 5 Polypay sheep given the higher dose of Ken06 died from acute RVFV infection following peak viremia, with all animals showing dramatic increases in AST levels and severe liver lesions. Increased BUN values in some of the animals following infection are consistent with kidney involvement. Importantly, RVFV antigen was detected in the kidney of one sheep inoculated with Ken06 in the virus comparison study and in several kidneys from sheep in the higher dose study.

Genome sequence analysis revealed sequence differences between the two challenge isolates, SA01 and Ken06. Notably, sequences of the non-structural protein, NSs, were the most variable between the two strains (see data in Results), which is consistent with previous findings of high variability of this gene among phleboviruses (Sall et al., 1997). Given the role of NSs as a major virulence factor for RVFV (Bouloy et al., 2001; Billecocq et al., 2004; Le May et al., 2008; Habjan et al., 2009; Ikegami et al., 2009), variability within its amino acid sequences could possibly account for the phenotypic differences between different virus strains.

Sheep exposed to both viral strains manifested serological responses to infection. The onset of seroconversion determined by N-specific IgG antibody ELISA (Faburay et al., 2013; Paweska et al., 2008a) was at 5 dpi in response to infection with both virus strains (Fig. 4A, B and D). Overall, both N-specific and Gn-specific antibody responses manifested a similar trend of increasing titers over time, although higher antibody activity was detected in the N-specific ELISA compared to the Gn-ELISA. These results corroborate the findings of other studies that demonstrate early-onset and strong antibody response to N protein upon RVFV infection (Faburay et al., 2013; Jansen van Vuren et al., 2007; Paweska et al., 2008b). The RVFV nucleocapsid protein is the most abundant viral protein and considered a suitable diagnostic antigen for detecting RVFV infection and monitoring vaccination with attenuated or inactivated viruses (Faburay et al., 2014, 2013). Although the majority of Dorper x Katahdin cross inoculated with either virus developed neutralizing antibody titers at 3 dpi, titers correlating with protection ($\geq$ 1:40) (Pittman et al., 2000) were only detected starting on 4 and 5 dpi, following appearance of acute clinical symptoms (fever) and viremia regardless of breed. The induction of neutralizing antibody response indicated host response to experimental virulent infection, and with the increase in neutralizing antibody titers over time (from 5 dpi onwards; Tables 1 and 2) resulted in suppression of virus replication and clearance of virus from the serum and tissues.

Although no infectious virus was detected in the serum of surviving animals after 5 dpi (Fig. 2B and D), the occurrence of viremia allows virus dissemination to peripheral organs, including liver and spleen as observed in these studies; and virus could be isolated from these tissues at 3–5 dpi (liver) and up to 21 dpi (spleen) of Dorper x Katahdin crossbred sheep inoculated with Ken06 (Fig. 3B, D and F). Isolation of low amounts of infectious virus from the liver and spleen after 6 dpi was supported by detection of viral nucleic acid in these tissues at the same time period (Fig. 3C and D). This suggests that animals recovering from virulent infection may harbor low levels of virus for an extended period of time in tissues, especially in the spleen, further indicating the utility of these tissues as useful diagnostic specimens for the diagnosis of RVF and for vaccine studies. The isolation of RVFV from organs and tissues of infected animals after appearance of clinical symptoms poses some potential risk of contact contamination, and could account for human (notably veterinarians and abattoir workers) infections (Swanepoel and Coetzer, 1994).

Conclusion

This is the first study that compared the pathogenesis of two genetically distinct virulent strains of RVFV (SA01 and Ken06) in a ruminant model, the sheep. It also represents the first study in a ruminant challenge model to demonstrate a peracute form of RVF caused by one of the wild type strains (Ken06). The findings suggest that genetic diversity between strains of RVFV can manifest in phenotypic differences. Sheep, the livestock species naturally most susceptible to RVFV, represents a relevant large animal model for RVF studies. The major clinical and pathological features, such as viremia, fever, hepatitis and hepatic necrosis were consistently reproduced in this host. Furthermore, this animal model could be used to understand RVFV pathogenesis and RVFV-induced pathology. The two genetically distinct viruses used in the present study (Ken06 and SA01) showed phenotypic differences, with Ken06 manifesting higher virulence in the Dorper x Katahdin cross. Genome sequence analysis revealed significant nucleotide and amino acid differences between the two RVFV strains (Ken06 and SA01), separating them into distinct genetic clades in the phylogenetic tree (Fig. 5). The observed variability in the level of clinical and pathological responses in different sheep breeds suggests potential breed influences on the clinical and pathological outcome of RVFV infection. Future studies should be directed at understanding the susceptibility of different US sheep breeds to RVFV infection and the influence of the viral genotype on virus virulence in natural hosts.

Materials and methods

Virus strains and cell culture

The RVFV Saudi Arabia 2001-1322 (SA01) (Miller et al., 2002) and Kenya 2006-128b-15 (Ken06) (Sang et al., 2010) were used as challenge isolates and were provided by R. Bowen, Colorado State University through B. Miller, Centers for Disease Control, Fort Collins, CO. The two virus strains were propagated in a C6/36 *Aedes albopictus* cell line (ATCC, Manassas, VA) with MEM culture medium (Life Technologies, Grand Island, NY) supplemented with 10% fetal bovine serum (FBS; Sigma-Aldrich, St. Louis, MO) and 1x Penicillin/Streptomycin/Fungizone (PSF; Gibco, USA) and maintained at 28 °C in sealed flasks; infected cells were maintained at 37 °C. The inocula were prepared from the first passage. MP12 is a non-virulent strain of RVFV, attenuated via chemical mutagenesis (Caplen et al., 1985), and was used as the viral stock in plaque reduction neutralization assays. For virus isolation and titration, the Vero MARU (Middle America Research Unit, Panama) cell line was used. Vero MARU cells were grown in Medium M-199 (M199E) culture medium (Sigma-Aldrich) supplemented with 10% FBS and 1xPSF, and maintained in a 37 °C, 5% CO_2 incubator.

Animals and experimental design

Fourteen healthy 4–5 month old sheep (*Dorper x Katahdin cross*), were obtained from a private breeder in Kansas, USA. None of the sheep had prior exposure to RVFV infection. The animals were acclimatized for seven days at the Large Animal Research Center (LARC; Kansas State University) prior to relocation to a BSL-3Ag facility at the Kansas State University Biosecurity Research Institute. In BSL-3Ag, the animals were divided into two experimental groups ($n=6$ per group). Two animals served as mock inoculation controls. The sheep were inoculated subcutaneously with 2 ml of 1×10^6 plaque forming units (PFU) of the Ken06 or SA01 virus, or an equivalent volume of media, respectively. Post inoculation, on days 0–10, 14 and 21 post infection (pi), all animals were monitored daily for clinical signs including rectal temperature. Nasal swabs for virological analysis and blood samples for virological, immunological, hematological and blood chemistry analyses were collected. One sheep per experimental group was euthanized and necropsied at 3, 4, 5, 6, 10 and 21 days post infection (dpi). The two mock-inoculated control sheep were necropsied at 21 dpi. Tissues were collected for viral titration and histopathology. In a follow-up experiment, 5 Polypay sheep, aged 4–5 months, were each inoculated with 2×10^6 PFU of Ken06 subcutaneously. Monitoring of clinical parameters (rectal temperatures, viremia and tissue viral load) was performed from day 0 through day 10 pi; tissues for virus titration and histopathology were also collected. Research was performed under an Institutional Animal Care and Use Committee-approved protocol of Kansas State University in compliance with the Animal Welfare Act and other regulations relating to animals and experiments involving animals.

Virus titration

Tissue samples of liver, spleen and bile were collected at necropsy and frozen at −80 °C. Approximately 10 mg of tissue was added to 1 ml M199E supplemented with 10% fetal bovine serum (FBS) and 1xpenicillin streptomycin fungizone (PSF), and homogenized by high-speed shaking dissociation with steel beads using the TissueLyser instrument (QIAGEN Inc., Valencia, CA). Virus challenge material, sheep sera, nasal swabs, bile and homogenized tissue samples were titrated by standard plaque assay on Vero MARU cells. Briefly, confluent cell monolayers were inoculated with ten-fold serially diluted samples in M199E and incubated for 1 h. Following adsorption, the inocula were replaced with a 1:1 mixture of 2% carboxymethyl cellulose (Sigma-Aldrich, St. Louis) in 2x M199E (20% FBS and 2xPSF) and returned to the incubator. After 5 days, cells were fixed and stained with crystal violet fixative (25% formaldehyde, 10% ethanol, 5% acetic acid, 1% crystal violet). Virus titers were calculated as plaque forming units per ml (pfu/ml).

Viral RNA extraction and real-time RT-PCR

Total RNA from serum, nasal swabs or homogenated tissue samples was extracted using TRIzol-LS reagent (Life Technologies, Grand Island, NY) and the magnetic-bead capture MagMAX-96 total RNA Isolation kit (Life Technologies). Briefly, 100 µl of aqueous phase was added to 90 µl of isopropanol and 10 µl bead mix. Total sample RNA was washed four times with wash buffer (150 µl), then eluted in 30 µl of elution buffer. A published quadruplex real-time reverse transcriptase-polymerase chain reaction (RT-PCR) assay was used to detect each of the three RVFV RNA genome segments (Wilson et al., 2013).

Viral RNA sequencing and phylogenetic analysis

To determine the genomic sequences of the two virus strains, 6 µl of viral RNA was reverse-transcribed using SuperScript III First-Strand Synthesis SuperMix (Invitrogen, Carlsbad, CA) and amplified using Platinum PCR SuperMix High Fidelity (Invitrogen, Carlsbad, CA). The optimized cycle conditions for cDNA synthesis were 50 °C for 70 min and 85 °C for 5 min and optimized cycle conditions for PCR were 94 °C for 3 min, 45 cycles of 94 °C for 30 sec, 54 °C for 30 s and 68 °C for 4 min followed by final extension at 68 °C for 10 min. All gene segments were amplified in two overlapping fragments (primer sequences are available on request). The amplified PCR products were then gel purified using QIAquick gel extraction kit (Qiagen, Valencia, CA). All six amplified gene fragments were pooled in equal copy number ratios and diluted to 0.2 ng/µl. One nanogram of pooled DNA was used for sequencing library preparation using the Illumina Nextera XT DNA library preparation kit (Illumina, San Diego, CA). The pooled barcoded libraries were sequenced on an Illumina MiSeq platform using paired 150 bp chemistry. Reads for each sample were parsed into individual files based on barcoded sequences. Parsed reads were loaded into CLC Genomic software package (Qiagen, Valencia, CA). Reads were *de novo* assembled and contigs were BLASTed against the Genbank nucleotide database. Consensus sequence for each strain was obtained from contigs that matched known Rift Valley fever virus genomes. For phylogenetic analysis, nucleotide sequences of the M segment of different RVFV strains were retrieved from GenBank (National Center for Biotechnology Information, Bethesda, USA). These sequences were aligned with the M segment nucleotide sequences of SA01 and Ken06 using MegAlign (DNAStar Inc, Madison, USA) program by method of ClustalW algorithm. A phylogenetic tree was constructed applying the sequence alignment by neighbor-joining method using the MegAlign software; and to infer tree robustness, 1000 bootstrap replicates were computed.

RVFV serology

Anti-RVFV IgG antibody response

Anti-RVFV antibody response was measured by an anti-RVFV total IgG indirect enzyme linked immunosorbent assay (ELISA) using recombinant baculovirus expressed RVFV Gn and N proteins as the diagnostic antigens as described previously (Faburay et al., 2013; Fafetine et al., 2007; Paweska et al., 2008a). The cut-off point for the specific ELISAs was determined by the addition of three

standard deviations to the corresponding mean *OD* value of the pre-vaccination serum. Mean *OD* values equal to or greater than the cut-off value were considered positive seroconversion.

Plaque reduction neutralization test (PRNT80)

To assess anti-RVFV neutralizing antibody response to RVFV infection, a plaque reduction neutralization test was performed as previously described (Faburay et al., 2014). Briefly, the stock of MP12 RVFV was diluted to 50 PFU in 250 μl of 1x MEM containing 4% bovine serum albumin (Sigma-Aldrich, St. Louis, MO). Separately, aliquots of serum from each vaccinated sheep were diluted as follows: 1:10, 1:20, 1:40, 1:80, 1:160, 1:320, 1:640 and 1:1280 in 1x MEM containing 2% bovine serum albumin and 1% penicillin streptomycin. Diluted serum (250 μl) was mixed with an equal volume of diluted MP12 virus and incubated at 37 °C for 1 h. Thereafter, each mixture of serum plus RVFV was used to infect confluent monolayers of Vero E6 cells in 12-well plates. After 1 h adsorption at 37 °C and 5% CO_2, the mixture was removed, and 1.5 ml of nutrient agarose overlay (1x MEM, 4% bovine serum albumin and 0.9% SeaPlaque agar) was added to the monolayers. After 4 days incubation, the cells were fixed with 10% neutral buffered formalin for 3 h prior to removal of the agarose overlay. The monolayer was stained with 0.5% crystal violet in PBS, and plaques were enumerated. The calculated $PRNT_{80}$ corresponded to the reciprocal titer of the highest serum dilution, which reduced the number of plaques by 80% or more relative to the virus control. As positive neutralizing serum control, a 1:40 dilution of day 28 neutralizing serum (titer $>$ 1280) obtained from a sheep previously immunized with the RVFV glycoprotein subunit vaccine was used (Faburay et al., 2014).

Hematology and blood chemistry analyses

Whole blood was added to K_2 EDTA tubes (Becton- Dickinson, Franklin Lakes, NJ) for complete blood count (CBC) determinations using a VetScan HM5 Hematology Analyzer (Abaxis, Union City, CA) according to the manufacturer's instructions. Clinical blood chemistry analyses examined the levels of albumin, alkaline phosphatase (ALP), gamma-glutamyl transferase (GGT), aspartate aminotransferase (AST) and blood urea nitrogen (BUN) in Lithium heparinized blood on a VetScan VS2 Chemical Analyzer (Abaxis, Union City, CA) according to manufacturer's instructions. Normal ranges for these chemistry values in sheep as specified by the manufacturer were used as reference values.

Pathology

For the first study in Dorper x Katahdin sheep, samples of the following tissues were collected at necropsy and placed in 10% neutral buffered formalin for at least 7 days: heart, lungs, trachea, thymus, liver, gall bladder, spleen, pancreas, kidney, adrenal gland, testicle, epididymis, salivary gland, thyroid gland, skeletal muscle and skin from the inoculation site, urinary bladder, small and large intestine, mesenteric lymph node, rumen, abomasum and eye. For the sheep in the second study, liver, spleen, eye, kidney and mesenteric lymph node were collected similarly.

For both studies, tissue samples were further trimmed, placed in cassettes, dehydrated and embedded in paraffin. All histochemical stains and immunohistochemistry were done on 5-μm sections placed on positively charged slides. Hematoxylin-and-eosin (H&E) stained tissues for the first study were independently reviewed by two veterinary pathologists in a blinded fashion and the liver pathology scored for lesion severity on a semi-quantitative scale from 0 to 3, where 0 signified no lesions and 1–3 progressively more severe pathology with a greater degree of liver involvement. A detailed definition of this scale is outlined in Table 3. Likewise the tissues were reviewed and liver lesions similarly scored on the same scale for the 5 second study sheep.

Immunohistochemistry (IHC) for RVFV antigen using the polyclonal rabbit anti-RVFV nucleocapsid protein antibody (Drolet et al., 2012) was conducted on all liver and spleen selections as well as additional tissue types where warranted by presence of lesions. Briefly, slides were deparaffinized and rehydrated, antigen was retrieved in pH 9.0 EDTA buffer, Bond ER Solution 2 (Leica Microsystems, Buffalo Grove, IL) for 10 min at 100 °C on the Leica Bond-Max autostainer (Leica Microsystems), incubated first for 15 min at RT with 1:1000 dilution of primary antibody and then for 25 min at RT with Anti-rabbit Poly-HRP-IgG (Leica Microsystems) with intermediary Bond Wash Solution (Leica Microsystems) rinses. Thereafter slides were washed in deionized water, blocked with 3% hydrogen peroxide diluted in water for 5 min, visualized with Mixed 3,3'-diaminobenzidine (DAB) Refine (Leica Microsystems), then counterstained with hematoxylin, and mounted in Acrymount (StatLab, McKinney, TX). Since samples yielded unsightly background by the automated IHC technique, a set of samples was additionally labeled by a different IHC detection technique (Vestastain Elite ABC Kit, Vector Labs, Burlingame, CA). Briefly, slides were deparaffinized and rehydrated, antigen retrieved using a vegetable steamer technique in pH 6.0 citrate buffer with detergents (DAKO, Carpinteria, CA) for 20 min, blocked with 3% hydrogen peroxide for 10 min, serum blocked as per kit, incubated overnight at 4 °C with 1:1000 dilution of primary antibody, secondary antibody and ABC reagent applied as per kit, and DAB followed by DAB Enhancing Solution applied as per vendor instructions (Vector Labs), counterstained with hematoxylin, and mounted in Permount (Electron Microscopy Systems, Hatfield, PA). Throughout, the following controls were employed, reagent control slides, with and without equivalent concentrations of primary antibody matched animal serum and uninfected control animal tissues. All gross tissue images were captured with a Canon G12 camera (Cannon, USA Inc, Melville, NY) and microscopic images were captured with a DP25 camera (Olympus, Tokyo, Japan) on a BX46 light microscope (Olympus) using CellSens Standard version 1.12 (Olympus). All microscopic images were further color calibrated using ChromaCal software ver 2.1 (Datacolor Inc., Lawrenceville, NJ) as per manufacturer's instructions and published recommendations (Linden et al., 2015).

Statistical analysis

Differences in values of key experimental parameters were analyzed statistically. Due to large variations in AST values among animals owing to variable individual animal responses to experimental inoculation, geometric mean values were derived for each group at each time point. Also group or individual mean values for temperature and BUN levels per time point were derived. The values were analyzed by One-Way Analysis of Variance (ANOVA) for independent samples followed by post hoc Tukey's Honest Significant Difference test. Differences in neutralizing antibody titers induced by the two wild type strains, Ken06 and SA01, were determined by *t*-test for independent samples with the neutralizing titer of 1280 considered highest; titers were tested for days 3–21 pi.

Acknowledgments

The authors wish to thank the staff of Kansas State University (KSU) Biosecurity Research Institute, the Comparative Medicine Group, and the staff of the Histopathology Unit at the Veterinary

Diagnostic Laboratory. Additionally, we wish to thank Dane Jasperson, Lindsey Reister, Chester McDowell, Tammy Koopman, Haixia Liu, Maira Cotton-Caballero, Elizabeth Stietzle, Monica Gamez and Mal Hoover for technical assistance. This work was funded by Grants of the Department of Homeland Security Center of Excellence for Emerging and Zoonotic Animal Diseases (CEEZAD), Grant no. 2010-ST061-AG0001, USDA Agricultural Services Project 5430-050-005-00D and Kansas State NBAF Transition Funds.

References

Al-Hazmi, M., Ayoola, E.A., Abdurahman, M., Banzal, S., Ashraf, J., El-Bushra, A., Hazmi, A., Abdullah, M., Abbo, H., Elamin, A., Al-Sammani el, T., Gadour, M., Menon, C., Hamza, M., Rahim, I., Hafez, M., Jambavalikar, M., Arishi, H., Aqeel, A., 2003. Epidemic Rift Valley fever in Saudi Arabia: a clinical study of severe illness in humans. Clin. Infect. Dis. 36 (3), 245–252.

Arishi, H., Ageel, A., Rahman, M.A., Hazmi, A.A., Arishi, A.R., Ayoud Menon, B., al., e., 2000. Outbreak of Rift Valley fever-Saudi Arabia, August–October, 2000. MMWR Morb. Mortal. Wkly. Rep. 49, 905–908.

Balkhy, H.H., Memish, Z.A., 2003. Rift Valley fever: an uninvited zoonosis in the Arabian Peninsula. Int. J. Antimicrob. Agents 21, 153–157.

Billecocq, A., Spiegel, M., Vialat, P., Kohl, A., Weber, F., Bouloy, M., Haller, O., 2004. NSs protein of Rift Valley fever virus blocks interferon production by inhibiting host gene transcription. J. Virol. 78, 9798–9806.

Bird, B.H., Albariño, C.G., Hartman, A.L., Erickson, B.R., Ksiazek, T.G., Nichol, S.T., 2008. Rift Valley Fever Virus lacking the NSs and NSm genes is highly attenuated, confers protective immunity from virulent virus challenge, and allows for differential identification of infected and vaccinated animals. J. Virol. 82 (6), 2681–2691.

Bird, B.H., Ksiazek, T.G., Nichol, S.T., Maclachlan, N.J., 2009. Rift Valley fever virus. J. Am. Vet. Med. Assoc. 234, 883–893.

Bird, B.H., Maartens, L.H., Campbell, S., Erasmus, B.J., Erickson, B.R., Dodd, K.A., Spiropoulou, C.F., Cannon, D., Drew, C.P., Knust, B., McElroy, A.K., Khristova, M.L., Albarino, C.G., Nichol, S.T., 2011. Rift Valley fever virus vaccine lacking the NSs and NSm genes is safe, nonteratogenic, and confers protection from viremia, pyrexia, and abortion following challenge in adult and pregnant sheep. J. Virol. 85 (24), 12901–12909.

Bouloy, M., Janzen, C., Vialat, P., Khun, H., Pavlovic, J., Huerre, M., Haller, O., 2001. Genetic evidence for an interferon-antagonistic function of rift valley fever virus nonstructural protein NSs. J. Virol. 75, 1371–1377.

Busquets, N., Lorenzo, G., Lopez-Gil, E., Rivas, R., Solanes, D., Galindo-Cardiel, I., Abad, F.X., Rodriguez, F., Bensaid, A., Warimwe, G., Gilbert, S.C., Domingo, M., Brun, A., 2014. Efficacy assessment of an MVA vectored Rift Valley Fever vaccine in lambs. Antivir. Res. 108, 165–172.

Busquets, N., Xavier, F., Martin-Folgar, R., Lorenzo, G., Galindo-Cardiel, I., del Val, B.P., Rivas, R., Iglesias, J., Rodriguez, F., Solanes, D., Domingo, M., Brun, A., 2010. Experimental infection of young adult European breed sheep with Rift Valley fever virus field isolates. Vector Borne Zoonotic Dis. 10 (7), 689–696.

Caplen, H., Peters, C.J., Bishop, D.H., 1985. Mutagen-directed attenuation of Rift Valley fever virus as a method for vaccine development. J. Gen. Virol. 66 (Pt 10), 2271–2277.

Chevalier, V., Pepin, M., Plee, L., Lancelot, R., 2010. Rift Valley fever–a threat for Europe? Euro Surveill. 15 (10), 19506.

Coetzer, J.A., 1977. The pathology of Rift Valley fever. I. Lesions occurring in natural cases in new-born lambs. Onderstepoort J. Vet. Res. 44 (4), 205–211.

Coetzer, J.A., 1982. The pathology of Rift Valley fever. II. Lesions occurring in field cases in adult cattle, calves and aborted foetuses. Onderstepoort J. Vet. Res. 49 (1), 11–17.

Daubney, R., Garnham, P., 1931. Enzootic hepatitis or Rift Valley fever. An undescribed virus disease of sheep, cattle and man from East Africa. J. Pathol. Bacteriol. 34, 545–579.

Drolet, B.S., Weingartl, H.M., Jiang, J., Neufeld, J., Marszal, P., Lindsay, R., Miller, M.M., Czub, M., Wilson, W.C., 2012. Development and evaluation of one-step rRT-PCR and immunohistochemical methods for detection of Rift Valley fever virus in biosafety level 2 diagnostic laboratories. J. Virol. Methods 179 (2), 373–382.

Easterday, B.C., 1965. Rift Valley fever. Adv. Vet. Sci. 10, 65–127.

Faburay, B., Lebedev, M., McVey, D.S., Wilson, W., Morozov, I., Young, A., Richt, J.A., 2014. A glycoprotein subunit vaccine elicits a strong Rift Valley fever virus neutralizing antibody response in sheep. Vector Borne Zoonotic Dis. 14, 746–756.

Faburay, B., Wilson, W., McVey, D.S., Drolet, B.S., Weingartl, H., Madden, D., Young, A., Ma, W., Richt, J.A., 2013. Rift Valley fever virus structural and nonstructural proteins: recombinant protein expression and immunoreactivity against antisera from sheep. Vector Borne Zoonotic Dis. 13 (9), 619–629.

Fafetine, J.M., Tijhaar, E., Paweska, J.T., Neves, L.C., Hendriks, J., Swanepoel, R., Coetzer, J.A., Egberink, H.F., Rutten, V.P., 2007. Cloning and expression of Rift Valley fever virus nucleocapsid (N) protein and evaluation of a N-protein based indirect ELISA for the detection of specific IgG and IgM antibodies in domestic ruminants. Vet. Microbiol. 121 (1–2), 29–38.

Fagbami, A.H., Tomori, O., Fabiyi, A., Isoun, T.T., 1975. Experimental Rift Valley fever in West African Dwarf sheep. Res. Vet. Sci. 18 (3), 334–335.

Findlay, G.M., 1932. Rift Valley fever or enzootic hepatitis. Trans. R. Soc. Trop. Med. Hyg. 25, 229–265.

Flick, R., Bouloy, M., 2005. Rift Valley fever virus. Curr. Mol. Med. 5, 827–834.

Habjan, M., Pichlmair, A., Elliott, R.M., Overby, A.K., Glatter, T., Gstaiger, M., Superti-Furga, G., Unger, H., Weber, F., 2009. NSs protein of rift valley fever virus induces the specific degradation of the double-stranded RNA-dependent protein kinase. J. Virol. 83 (9), 4365–4375.

Heald, R., 2012. Infectious disease surveillance update: Rift Valley fever in Mauritania. Lancet Infect. Dis. 12, 915.

Ikegami, T., Makino, S., 2011. The Pathogenesis of Rift Valley fever. Viruses 3, 493–519.

Ikegami, T., Narayanan, K., Won, S., Kamitani, W., Peters, C.J., Makino, S., 2009. Rift Valley fever Virus NSs protein promotes post-transcriptional downregulation of protein kinase PKR and inhibits eIF2α phosphorylation. Plos. Pathog. 5 (2), e1000287.

Iranpour, M., Turell, M.J., Lindsay, L.R., 2011. Potential for Canadian mosquitoes to transmit Rift Valley fever virus. J. Am. Mosq. Control. Assoc. 27 (4), 363–369.

Jansen van Vuren, P., Potgieter, A.C., Paweska, J.T., van Dijk, A.A., 2007. Preparation and evaluation of a recombinant Rift Valley fever virus N protein for the detection of IgG and IgM antibodies in humans and animals by indirect ELISA. J. Virol. Methods 140 (1–2), 106–114.

Kortekaas, J., Antonis, A.F., Kant, J., Vloet, R.P., Vogel, A., Oreshkova, N., de Boer, S.M., Bosch, B.J., Moormann, R.J., 2012. Efficacy of three candidate Rift Valley fever vaccines in sheep. Vaccine 30 (23), 3423–3429.

Le May, N., Mansuroglu, Z., Leger, P., Josse, T., Blot, G., Billecocq, A., Flick, R., Jacob, Y., Bonnefoy, E., Bouloy, M., 2008. A SAP30 complex inhibits IFN-beta expression in Rift Valley fever virus infected cells. Plos. Pathog. 4 (1), e13.

Linden, M.A., Sedgewick, G.J., Ericson, M., 2015. An innovative method for obtaining consistent images and quantification of histochemically stained specimens. J. Histochem. Cytochem. 63 (4), 233–243.

Madani, T.A., Al-Mazrou, Y.Y., Al-Jeffri, M.H., Mishkhas, A.A., Al-Rabeah, A.M., Turkistani, A.M., Al-Sayed, M.O., Abodahish, A.A., Khan, A.S., Ksiazek, T.G., Shobokshi, O., 2003. Rift Valley fever epidemic in Saudi Arabia: epidemiological, clinical and laboratory characteristics. Clin. Infect. Dis. 37 (8), 1084–1092.

Miller, B.R., Godsey, M.S., Crabtree, M.B., Savage, H.M., Al-Mazrao, Y., Al-Jeffri, M.H., Abdoon, A.M., Al-Seghayer, S.M., Al-Shahrani, A.M., Ksiazek, T.G., 2002. Isolation and genetic characterization of Rift Valley fever virus from Aedes vexans arabiensis, Kingdom of Saudi Arabia. Emerg. Infect. Dis. 8 (12), 1492–1494.

Nguku, P.M., Sharif, S.K., Mutonga, D., Amwayi, S., Omolo, J., Mohammed, O., Farnon, E.C., Gould, L.H., Lederman, E., Rao, C., Sang, R., Schnabel, D., Feikin, D.R., Hightower, A., Njenga, M.K., Breiman, R.F., 2010. An investigation of a major outbreak of Rift Valley fever in Kenya: 2006–2007. Am. J. Trop. Med. Hyg. 83 (2 Suppl), 5–13.

Nicholas, D.E., Jacobsen, K.H., Waters, N.M., 2014. Risk factors associated with human Rift Valley fever infection: systematic review and meta-analysis. Trop. Med. Int. Health 19 (12), 1420–1429.

Paweska, J., van Vuren, P., Kemp, A., Buss, P., Bengis, R., Gakuya, F., Breiman, R., Njenga, M., Swanepoel, R., 2008a. Recombinant nucleocapsid-based ELISA for detection of IgG antibody to Rift Valley fever virus in African buffalo. Veter-Microbiol. 127, 21–28.

Paweska, J.T., van Vuren, P.J., Kemp, A., Buss, P., Bengis, R.G., Gakuya, F., Breiman, R.F., Njenga, M.K., Swanepoel, R., 2008b. Recombinant nucleocapsid-based ELISA for detection of IgG antibody to Rift Valley fever virus in African buffalo. Vet. Microbiol. 127 (1-2), 21–28.

Pepin, M., Tordo, N., 2010. Emerging and re-emerging animal viruses. Foreword. Vet. Res. 41 (6), 69.

Pittman, P., Liu, C., Cannon, T., Makuch, R., Mangiafico, J., Gibbs, P., Peters, C., 2000. Immunogenicity of an inactivated Rift Valley fever vaccine in humans: a 12-year experience. Vaccine 18, 181–189.

Rippy, M.K., Topper, M.J., Mebus, C.A., Morrill, J.C., 1992. Rift Valley fever virus induced encephalomyelitis and hepataitis in calves. Vet. Pathol. 29 (6), 495–502.

Sall, A.A., de, A.Z.P.M., Zeller, H.G., Digoutte, J.P., Thiongane, Y., Bouloy, M., 1997. Variability of the NS(S) protein among Rift Valley fever virus isolates. J. Gen. Virol. 78, 2853–2858 (Pt 11).

Sang, R., Kioko, E., Lutomiah, J., Warigia, M., Ochieng, C., O'Guinn, M., Lee, J.S., Koka, H., Godsey, M., Hoel, D., Hanafi, H., Miller, B., Schnabel, D., Breiman, R.F., Richardson, J., 2010. Rift Valley fever virus epidemic in Kenya, 2006/2007: the entomologic investigations. Am. J. Trop. Med. Hyg. 83 (2 Suppl), 28–37.

Smith, D.R., Bird, B.H., Lewis, B., Johnston, S.C., McCarthy, S., Keeney, A., Botto, M., Donnelly, G., Shamblin, J., Albariño, C.G., Nichol, S.T., Hensley, L.E., 2012. Development of a Novel nonhuman primate model for Rift Valley Fever. J. Virol. 86 (4), 2109–2120.

Smith, D.R., Steele, K.E., Shamblin, J., Honko, A., Johnson, J., Reed, C., Kennedy, M., Chapman, J.L., Hensley, L.E., 2010. The pathogenesis of Rift Valley fever virus in the mouse model. Virology 407 (2), 256–267.

Swanepoel, R., Coetzer, J.A.W., 1994. Rift Valley Fever. In: Coetzer, J.A.W., Thomson, G.R., Tustin, R.C. (Eds.), Infectious Diseases of Livestock with Special Reference to Southern Africa., Vol. 1. Oxford University Press, UK, pp. 688–717.

Tomori, O., Kasali, O., 1979. Pathogenicity of different strains of Rift Valley fever virus in Swiss albino mice. Br. J. Exp. Pathol. 60 (4), 417–422.

Turell, M.J., Dohm, D.J., Mores, C.N., Terracina, L., Wallette Jr., D.L., Hribar, L.J., Pecor, J.E., Blow, J.A., 2008. Potential for North American mosquitoes to transmit Rift Valley fever virus. J. Am. Mosq. Control. Assoc. 24 (4), 502–507.

Turell, M.J., Wilson, W.C., Bennett, K.E., 2010. Potential for North American mosquitoes (Diptera: Culicidae) to transmit rift valley fever virus. J. Med. Entomol. 47 (5), 884–889.
Weingartl, H.M., Miller, M., Nfon, C., Wilson, W.C., 2014. Development of a Rift Valley fever virus viremia challenge model in sheep and goats. Vaccine 32 (20), 2337–2344.
Wilson, W.C., Bawa, B., Drolet, B.S., Lehiy, C., Faburay, B., Jasperson, D.C., Reister, L., Gaudreault, N.N., Carlson, J., Ma, W., Morozov, I., McVey, D.S., Richt, J.A., 2014. Evaluation of lamb and calf responses to Rift Valley fever MP-12 vaccination. Vet. Microbiol. 172 (1–2), 44–50.
Wilson, W.C., Romito, M., Jasperson, D.C., Weingartl, H., Binepal, Y.S., Maluleke, M.R., Wallace, D.B., van Vuren, P.J., Paweska, J.T., 2013. Development of a Rift Valley fever real-time RT-PCR assay that can detect all three genome segments. J. Virol. Methods 193 (2), 426–431.